Materials Science & Engineering A 639 (2015) 474–481

Contents lists available at ScienceDirect

Materials Science & Engineering A

journal homepage: www.elsevier.com/locate/msea

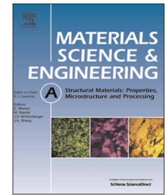

Exploring the mechanical strength of additively manufactured metal structures with embedded electrical materials

J. Li*, T. Monaghan, S. Masurtschak, A. Bournias-Varotsis, R.J. Friel, R.A. Harris

Wolfson School of Mechanical and Manufacturing Engineering, Loughborough University, Loughborough, Leicestershire LE11 3TU, UK

ARTICLE INFO

Article history:
Received 11 January 2015
Received in revised form
22 March 2015
Accepted 10 May 2015
Available online 18 May 2015

Keywords:
Ultrasonic Additive Manufacturing
3D printing
Layered manufacturing
Aluminium
Embedded electrical materials
Mechanical strength

ABSTRACT

Ultrasonic Additive Manufacturing (UAM) enables the integration of a wide variety of components into solid metal matrices due to the process induced high degree of metal matrix plastic flow at low bulk temperatures. Exploitation of this phenomenon allows the fabrication of previously unobtainable novel engineered metal matrix components.

The feasibility of directly embedding electrical materials within UAM metal matrices was investigated in this work. Three different dielectric materials were embedded into UAM fabricated aluminium metal-matrices with, research derived, optimal processing parameters. The effect of the dielectric material hardness on the final metal matrix mechanical strength after UAM processing was investigated systematically via mechanical peel testing and microscopy. It was found that when the Knoop hardness of the dielectric film was increased from 12.1 HK/0.01 kg to 27.3 HK/0.01 kg, the mechanical peel testing and linear weld density of the bond interface were enhanced by 15% and 16%, respectively, at UAM parameters of 1600 N weld force, 25 μm sonotrode amplitude, and 20 mm/s welding speed. This work uniquely identified that the mechanical strength of dielectric containing UAM metal matrices improved with increasing dielectric material hardness. It was therefore concluded that any UAM metal matrix mechanical strength degradation due to dielectric embedding could be restricted by employing a dielectric material with a suitable hardness (larger than 20 HK/0.01 kg). This result is of great interest and a vital step for realising electronic containing multifunctional smart metal composites for future industrial applications.

© 2015 The Authors. Published by Elsevier B.V. This is an open access article under the CC BY license (http://creativecommons.org/licenses/by/4.0/).

1. Introduction

Ultrasonic Additive Manufacturing (UAM) utilises Ultrasonic Metal Welding (UMW) to weld metal foils layer by layer, and then periodically applies Computer Numerical Control (CNC) machining to produce a 3D metal structure [1] (Fig. 1). During the UAM process, energy generated from an ultrasonic transducer is transferred to a work piece through a textured sonotrode in the form of ultrasonic oscillations. With a compressive normal force via the sonotrode, the oscillations cause friction/scrubbing at the mating surfaces; this disrupts oxide films at the interface and generates clean metal to metal contact points. Plastic deformation of nascent metal beneath the contact surfaces further helps the break-up of the oxide layer and the generation of further new clean contact points. The result of the compression and ultrasonic oscillation is a solid state weld resulting in true metallurgical bonding at the contact interface [2].

Due to two key abilities, UAM enables the integration of a wide variety of components into solid metal matrices. Firstly, UAM is a solid state bonding process and the bulk temperature increase during processing is normally lower than 50% of the melting point of the metals to be consolidated, which would avoid potential damage to thermally sensitive embedded components caused by thermal stress and melting [3]. Secondly, large plastic flow of the metal matrix during ultrasonic excitation permits the full encapsulation of inserted components [4]. In addition to the two key abilities of UAM the process is also faster than many other metal AM processes, so it is capable of building large metal components in a comparatively short period of time. Lastly, the UAM process can be paused in an ambient temperature and atmosphere and left for essentially any amount of time and then restarted again without adverse effects. This makes an ideal system for integrating electrical components into solid metal matrices in a layer-by-layer fashion.

With the UAM process, Kong et al. [5] and Mou et al. [6] successfully embedded optical fibre sensors into aluminium matrices. Furthermore, pre-packaged electronic systems and direct-written circuitries have also been encapsulated in UAM metal structures

* Corresponding author. Tel.: +44 1509227567.
E-mail address: J.Li5@lboro.ac.uk (J. Li).

http://dx.doi.org/10.1016/j.msea.2015.05.019
0921-5093/© 2015 The Authors. Published by Elsevier B.V. This is an open access article under the CC BY license (http://creativecommons.org/licenses/by/4.0/).

by Siggard et al. [7] and Robinson et al. [8], respectively. However, UAM embedded electronics at current state-of-art still have some limitations: (1) the electronic encasing and circuiting are still in 2D planar and no 3D freeform embedding capability has been demonstrated which restricted the range of applications and the freedom of design and manufacture; (2) the integration level of the metal structure was relatively low due to the large size of the embedded electronic components; (3) extra process steps such as milling protection pockets and channels for electronic components and padding them with epoxy were required which confounded the manufacturing process; (4) the large volume pockets and channels milled for electronics placement degraded the mechanical strength of the structure as a whole. Although this previous research has shown that electronics and sensor integration with UAM is possible it is pertinent to now explore an entirely new realm of multifunctional structures via the direct (i.e. with no extra process step such as pocket machining) integration of printed electronic techniques with UAM to possibly attain never before achieved multi-functional metal matrix composites.

To attain these multi-functional metal matrix composites the compatibility and effects of electronic materials with UAM must first be established. This paper documents the findings of that investigation of UAM embedded dielectric materials.

2. Experimental methodology

2.1. Materials

A 5 mm thick and 30 mm wide aluminium (Al) 1050 H14 plate was used as a base plate for the UAM process, and two Al 3003 H18 foils with a thickness and width of 100 μm and 24 mm respectively were ultrasonically welded onto the Al 1050 base plate to create the UAM metal matrices. The mechanical properties and chemical composition of Al 1050 and Al 3003 are summarised in Table 1 [9,10].

To identify the compatibility between UAM process and dielectric materials, a significant preliminary embedding experimentation was performed with a wide range of candidate dielectrics. It was found that the range of materials capable of actually being embedded via UAM was limited. Three identified dielectric inks, LuxPrint® 8153 from DuPont™, 520 Series Soldermask made by Technic, and Imagecure® AQ XV501T-4 of Sunchemical® were finally employed in this work. These inks are all commercial products that are widely used in the printed electronics industry. 8153 is a single part thermal curable ink for manufacturing screen-printed Electroluminescent (EL) lamps, while both 520 Series and XV501T-4 are two-component solder resists used in rigid printed circuit boards (PCBs). In tests, all three inks were solidified thermally as per the manufacturer's instructions and the parameters used are shown in Table 2 [11–13].

2.2. UAM apparatus

The UAM apparatus used in this research was the Alpha 2 UAM machine supplied by Solidica INC. (USA) as shown in Fig. 2. The Alpha UAM machine works with an input power of 20 kW and a constant frequency of ~20 kHz. Three control parameters of the apparatus, normal force (N), sonotrode amplitude (μm), and welding speed (mm/s), can be varied by users to adjust the energy applied to the workpieces. The normal force is the downward force of the sonotrode on the metal foil to be welded that permits close contact between metal foil and substrate, and can be varied from 100 N to 2000 N. The sonotrode amplitude refers to the longitudinal oscillatory displacement of the sonotrode that can be varied within a range

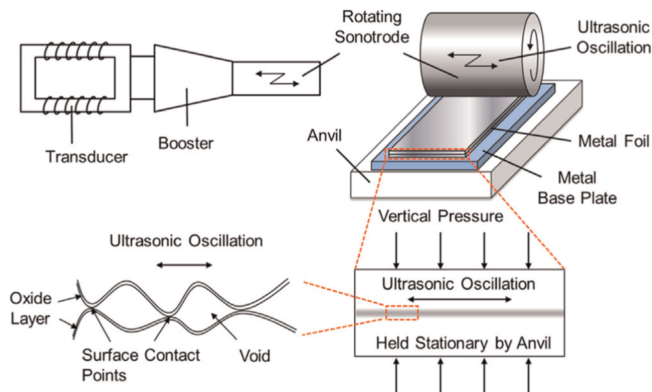

Fig. 1. Schematic drawing of Ultrasonic Additive Manufacturing (UAM).

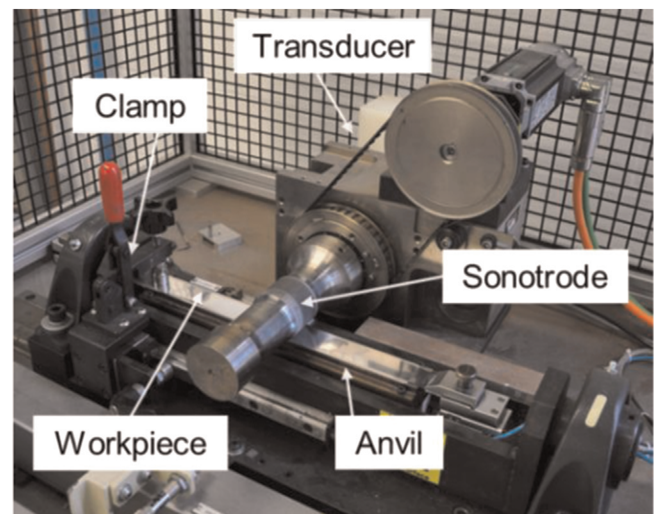

Fig. 2. Alpha 2 UAM Machine.

Table 1
Mechanical properties and chemical composition of Al 1050 H14 and Al 3003 H18.

	Al 1050 H14	Al 3003 H18
Density (g/cm^3)	2.71	2.73
UTS (MPa)	100–135	200
Tensile yield strength (MPa)	75	186
Elongation at break (%)	4–8	1–4
Modulus of elasticity (GPa)	69	68.9
Melting temperature (°C)	645–657	643–654
Composition (wt%)	Al (≥ 99.08), Mn (≤ 0.05), Cu (≤ 0.05), Fe (≤ 0.4), Si (≤ 0.25), Zn (≤ 0.07), Mg (≤ 0.05), Ti (≤ 0.05), Other (≤ 0.03)	Al (96.7–99), Mn (1–1.5), Cu (0.05–0.2), Fe (≤ 0.7), Si (≤ 0.6), Zn (≤ 0.1), Other (≤ 0.15)

of 10–25 μm. The welding speed defines sonotrode motion speed across the workpiece during welding. The welding speed can be varied from 1 mm/s up to 100 mm/s. The sonotrode is made of tool steel and has an average surface roughness R_a of 5.2 μm.

2.3. Sample preparation and topography characterisation

2.3.1. Process chain of test sample fabrication

The process chain of sample fabrication is demonstrated in Fig. 3. Firstly, two Al 3003 H18 foils were ultrasonically welded onto Al 1050 H14 base plate at room temperature (Fig. 3(a)). The UAM parameters used were 1600 N weld force, 25 μm sonotrode amplitude, and 20 mm/s welding speed, respectively, which were obtained via systematic tests and prior studies focusing on the UAM of 3003 H18 aluminium [14–16].

Dielectric films were then screen printed onto the aluminium substrates using a mesh screen and bespoke stencil via a DEK 265 Horizon printer. The printed dielectric layers were cured as recommended by the manufacturers (Table 2) and had the final dimensions: 38 mm long, 3 mm wide, and approx. 45 μm thick (Fig. 3(b)).

The screen printed dielectric layers were then encased by ultrasonically welding another Al 3003 H18 foil onto the substrate (Fig. 3(c)). Two combinations of control parameters with different UAM processing energy were applied in embedding: a high UAM energy combination 1600 N normal force, 25 μm sonotrode amplitude, and 20 mm/s welding speed; and a low UAM energy set: 800 N normal force, 15 μm sonotrode amplitude, and 10 mm/s welding speed. According to an analytical energy model built by Yang et al. [17], the energy density of high and low UAM energy combinations is 2 J/mm^2 and 1.2 J/mm^2, respectively. In this way, the effect of UAM processing energy on mechanical strength of the metal composite could be investigated. Samples with no dielectric material were also manufactured with both UAM parameter sets. These samples were used as a reference to evaluate any potential change of mechanical strength due to dielectric embedment.

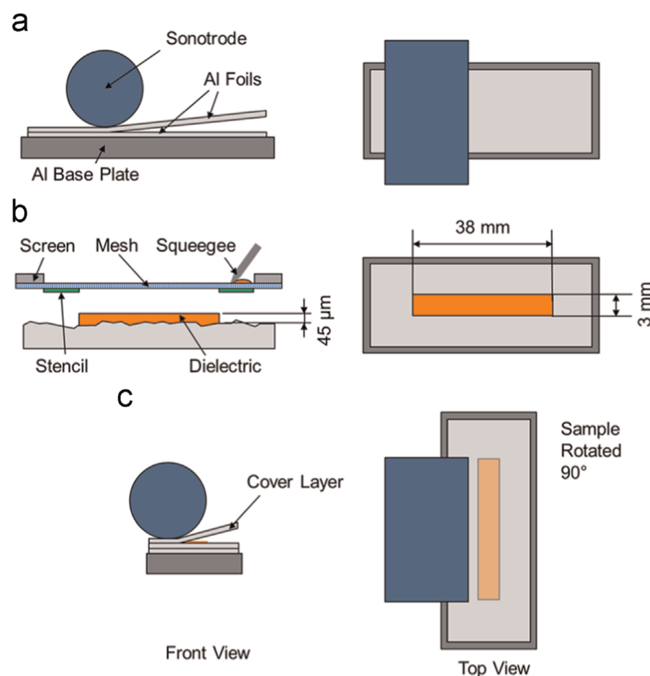

Fig. 3. Process chain of test sample preparation.

Table 2
Curing conditions of dielectric inks.

	LuxPrint® 8153	520 Series soldermask	Imagecure® AQ XV501T-4
Cure conditions (Box oven)	130 °C/10 min	120 °C/30–45 min	150 °C/60 min

Table 3
Talysurf CLI 2000 parameter settings.

Parameter	Setting
Gauge name	CLA Gauge
Vertical measurement range	300 μm
Real vertical measurement range	319.84 μm
Gauge resolution	36. 909 pm
Scanning line spacing (*X* axis)	8.75 mm
Scanning point spacing (*Y* axis)	0.5 μm
Scanning speed	200 μm/s
Sampling rate	500 Hz

2.3.2. Topography of aluminium substrates and dielectric films

To verify that the dielectric films were sufficiently thick to overcome the roughness of the UAM processed aluminium substrate to achieve electrical insulation, the surface topography of aluminium substrates with three different dielectric films were investigated by using Talysurf CLI 2000, a high-resolution 3D non-contact surface profiling systems, to scan the surfaces of the aluminium substrates with deposited dielectric films. The parameter settings used for measurement are stated in Table 3.

2.4. Effects of dielectric hardness on mechanical strength

To determine any possible effects of dielectric hardness on composite strength, three dielectric materials with different hardness were printed and embedded in the UAM interlaminar interface. The aspects of mechanical strength of UAM metal structures with embedded dielectric materials were systematically investigated via peel testing and optical microscopy. This allowed quantification of any dielectric hardness effect, in combination with encasing processing parameters, on UAM embedded samples.

2.4.1. Knoop hardness (HK) of dielectrics

Generally, hardness is a composite material property with contributions from the yield strength, work hardening, true tensile strength, modulus, and others factors. Therefore, it is an ideal index to describe the resistance of printed dielectrics to UAM load and the influence of material property on mechanical strength.

The hardness of the three dielectrics provided by manufactures was characterised by pencil hardness in accordance with ASTM D3363–05 which uses the hardness of pencil graphite as a measure of film hardness. This hardness is used more for a grade as opposed to a specific value and so for this investigation a more accurate method of hardness measurement was used.

The dielectric films were relatively thin ($<$ 50 μm) thus Knoop hardness testing was chosen due to it being better suited to thin coating microhardness measurement [18,19]. In the test procedure a load of 0.01 kg was applied on a rhombic-based diamond pyramid indenter to make an indentation which is measured and converted to a hardness value. Accordingly, the penetration depth of the indenter could be restricted within 10% of the film thickness to avoid the substrate influencing the results of the tests [20–22].

A Struers DuraScan 70 automatic hardness tester was used to measure the Knoop hardness of the dielectrics. Indentations were performed under load control mode that increased the load to a preset value and then held for a certain time to reduce the influence of creep. The maximum load applied to all three dielectrics was 0.01 kg and the load duration time was set to be 10 s. For each dielectric,

three printed samples were measured and 10 indentations were made on each sample. The Knoop hardness of the UAM processed aluminium substrate was also measured for reference.

2.4.2. Peel testing

Peel testing was performed in accordance with BS EN 2243-2 2005. By assessing samples' average resistance to peeling, the effect of dielectric hardness and UAM processing energy on mechanical strength could be analysed quantitatively. For each dielectric embedded with a certain parameter setting, three samples were peeled and the average peel load was calculated. Six samples with no dielectric film were also fabricated using both parameter combinations and tested in the same way to measure the peel strength of the metal matrix bond interface. Totally, 24 samples were prepared for peel testing. By comparing the peeling loads for the samples with and without dielectric films the mechanical strength degradation could be clearly revealed.

A peeling jig was installed to an Instron 3366 tensile test machine to peel samples that were mounted as shown in Fig. 4. The un-welded end of the cover foil used to load the sample was 100 ± 5 mm in length. In the peeling, 50 mm/min was used as the tensile loading speed and testing was set to stop when the extension of the free end of the foil reached 40 mm thus peeling off the cover foil completely from the dielectric area.

2.4.3. Optical weld density analysis

The potential influence of dielectric hardness and UAM processing energy on the mechanical strength was also investigated systematically via quantifying the density of bonding. A measurement technique was performed to measure and calculate the proportion of the direct bonded area by optically measuring microscopy images of embedment cross-sections. In this paper, Linear Weld Density (LWD) was used to describe the percentage of bonded area along the weld interface, the proportion of encased dielectric area to the total embedment interface and is expressed as:

$$\text{LWD}(\%) = \frac{L_b}{L_i} \times 100 \quad (1)$$

where L_b and L_i are the bonded area length and the bond interface length, respectively. Additionally, the Width of Embedment Area (WEA) was measured to indicating the region with no Al–Al bond.

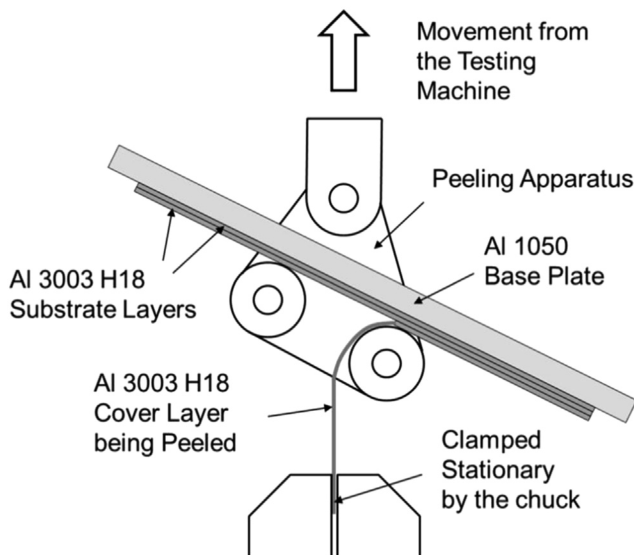

Fig. 4. Schematic drawing of a test sample mounted on a peeling jig.

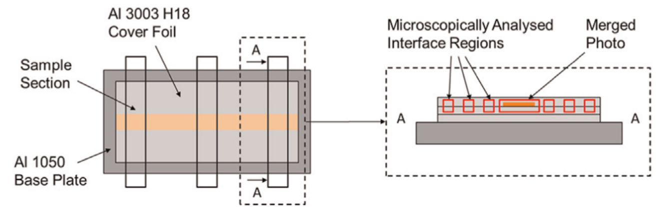

Fig. 5. Method of sample sectioning and microscopic analysis to determine the linear weld density and the width of embedding area.

Table 4
Topography of UAM processed aluminium substrates and dielectric films.

	520 Series	8153	XV501T-4	Aluminium substrate
R_a [μm]	1.4 ± 0.3	0.8 ± 0.2	0.2 ± 0.0	3.2 ± 0.8
R_z [μm]	6.8 ± 0.9	4.8 ± 0.9	1.5 ± 0.1	22.6 ± 4.4
Dielectric thickness [μm]	43.4 ± 1.0	47.8 ± 0.8	43.6 ± 0.5	–
Number of printed layers	3	4	3	–
Thickness of single layer [μm]	14–15	11–12	14–15	–

Samples of each dielectric embedded with a certain parameter combination were cross-sectioned and microscopically investigated. Four samples without dielectric film were also built for characterising the mechanical strength of aluminium matrices. Each sample was cut into front, middle and rear sections (Fig. 5) which were mounted in epoxy resin and then gradually ground and polished to 0.05 μm. In total 48 sections were prepared and investigated. An Olympus BX60M optical microscope with a × 100 magnification lens was used to take images for LWD calculation. For each mounted section, six images of weld interface were taken from both sides of the embedded dielectric. Merged photos were employed to obtain the width of embedment area.

3. Results and discussion

3.1. Topography of aluminium substrates and dielectric films

The surfaces of the samples with printed dielectrics were scanned using Talysurf CLI 2000 3D surface profiling systems, and the measured data was studied with TalyMap Platinum 5.0 software. The average roughness R_a and the maximum peak-to-valley distance R_z of both UAM processed aluminium substrate and the top surfaces of three dielectric films are stated in Table 4. The thickness, the number of printed layers, and the thickness of single printed layers of three dielectrics are also listed. To achieve electrical insulation, the dielectric film must overcome the roughness of the UAM processed aluminium substrate, thus the thickness of dielectric film needs to be larger than the maximum peak-to-valley distance of aluminium substrate. For 520 Series and XV501T-4 dielectric, at least two layers were needed to be deposited to neutralise the uneven substrate surface, while for 8153 three layers were demanded. In future work, dielectrics will be used to sandwich electrical conductive structures, so a dielectric cover layer should be taken into account which makes the final thickness of complete electrical device likely to be around 45 μm. Therefore, in this work all three dielectrics were deposited to approx. 45 μm to simulate the performance of future electrical devices during UAM embedding. Furthermore, compared with the aluminium substrate, the average roughness R_a of all three dielectric films was reduced by more than 50%. Glossy dielectric surfaces were desirable for depositing other electrical materials such as conductive

inks, because with limited printing strokes (one or two layer printing) continuous structures could be made.

Typical profiles of three dielectric films were plotted in Fig. 6. With the thickness of about 45 μm all three dielectric films entirely adapted the rough Al substrate (R_z:22.6 ± 4.4 μm) and provided much smoother top surfaces (Compared with Al substrate processed by UAM, R_a of dielectric surface was reduced by more than 50%.). The electrical insulation of the dielectric film was checked using a multimeter to measure the resistance between the front surface of dielectric film and Al substrate. No shorting was found for all three dielectrics in the test which also confirmed that the roughness of the UAM processed aluminium substrate had been overcome.

3.2. Effects of dielectric hardness on mechanical strength

3.2.1. Knoop hardness of printed dielectrics

Knoop hardness results of the dielectrics are shown in Fig. 7. The average Knoop hardness of 520 Series, XV501T-4 and 8153 were 27.3 HK/0.01 kg, 23.0 HK/0.01 kg and 12.1 HK/0.01 kg, respectively, while the UAM processed aluminium substrate was up to 76 HK/0.01 kg. The deepest indentation occurred with 8153 films. For a standard 172°30′ Knoop indenter, 12.1 HK/0.01 kg corresponded to a long diagonal of 108 μm and a penetration depth of ~3.6 μm that was less than 10% of the film thickness (~4.8 μm). Accordingly, there was no evidence of penetration of the micro-indenter through the dielectric film to the substrate and the films were therefore sufficiently thick for accurate microhardness measurements.

The 8153 film is ~10% thicker than the other dielectrics (Table 4) thus a series of Knoop hardness tests were conducted to explore the effects of film thickness on the dielectric hardness. 8153 films with thickness of 43 μm, 45 μm, 48 μm, 50 μm, and 54 μm were used for the measurements. For each thickness, two printed samples were used and 10 indentations were made on each sample. As the results show in Fig. 8, it was found that the measured Knoop hardness did not differ significantly with the varying thicknesses of 8153 dielectric film and the error bars of the measurements show a large degree of overlap. Therefore, in this case the effect of film thickness on dielectric hardness was found to be insignificant.

3.2.2. Peeling test

The peeling test was performed as described in Section 2.4.2. The average maximum peeling load for the three dielectric films embedded with two combinations of UAM parameters were plotted in Fig. 9.

For each combination of UAM process parameters, the peeling load increased with the dielectric hardness. Compared with the samples containing no dielectric the peeling load of hard dielectric (520 Series) dropped down slightly by about 10%, whereas for soft dielectric (8153) dramatic reduction (more than 1/3) was observed. It can be deducted that increasing the hardness of dielectric is capable of maximising the mechanical strength of UAM metal structure with embedded electrical materials.

For each dielectric, the samples encased with higher UAM process energy (1600 N force, 20 mm/s speed, and 25 μm) exhibited higher peeling loads than those made by lower UAM process energy (800 N force, 10 mm/s speed, and 15 μm). Moreover, there was a significant deviation on the peeling load of 8153 encased by low UAM process

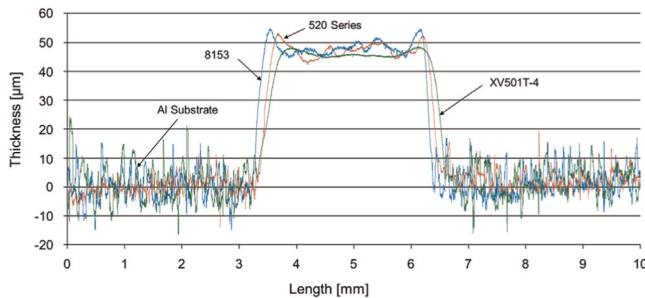

Fig. 6. Surface profiles of three dielectric films and aluminium substrate.

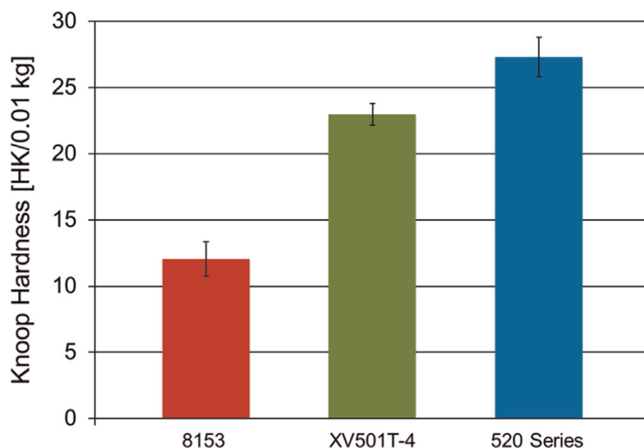

Fig. 7. Average Knoop hardness of the three dielectric films with standard deviations.

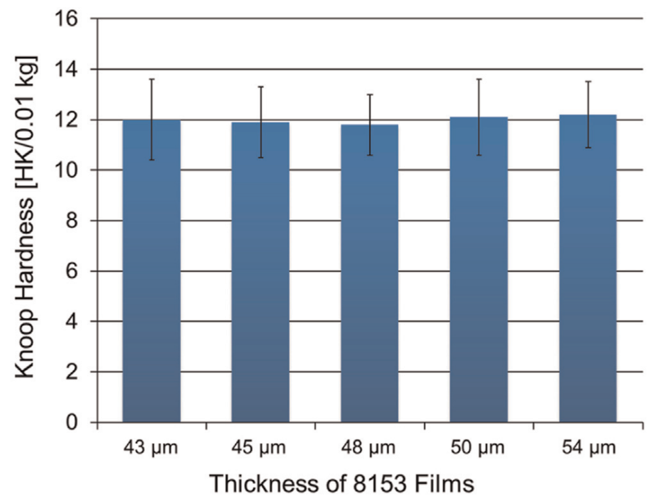

Fig. 8. Knoop hardness of the 8153 films with different thickness.

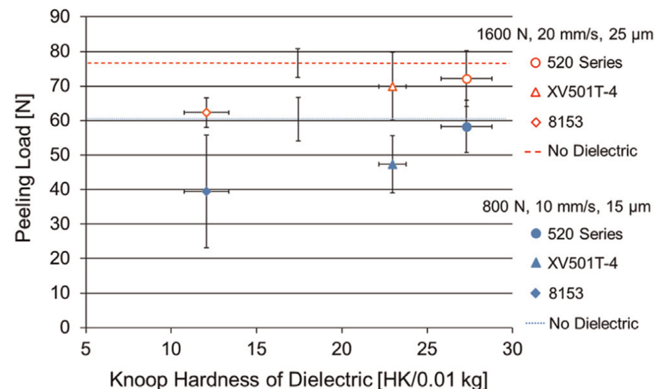

Fig. 9. The average maximum peeling loads for the three dielectric films embedded with two combinations of UAM parameters.

energy. These could be explained by the fragile mode of Al cover foils during the peeing test: brittle mode and ductile mode (Fig. 10). Brittle mode presented a clear fracture in the front of a weld area, while ductile mode illustrated a fracture due to the growth of breaking points under load. For most samples encased using high UAM process energy (including no-dielectric samples), a brittle failure mode was observed which provided high peeling loads of up to around 70 N, and ductile mode occurred in most of those made by low UAM process energy (including no-dielectric samples) giving a peeling loads less than 60 N. Accordingly, raising UAM energy is an effective method to strengthen mechanical performance of metal matrix composite.

3.3. Optical welding density analysis

As mentioned in Section 2.4.3, Linear Welding Density (LWD) and the Width of Embedment Area (WEA) were measured and then calculated for each dielectric via the microscopic analysis of cross-sections (Fig. 11). The average LWD and the average WEA are demonstrated graphically in Figs. 12 and 13, respectively.

The general tendency was that higher UAM processing energy and harder dielectric material resulted in a higher average LWD. It is noticeable that average LWD of 8153 embedded using low UAM processing energy also showed a large deviation in results. Both of these were in accordance with the peeling load.

According to Fig. 13, for high UAM processing energy average WEA could be reduced by using a harder dielectric. However, for low UAM processing energy average WEA did not change markedly and fluctuated around 5.5 mm. Besides, a large deviation of approx. 1.4 mm of WEA was found in the samples with 8153 embedded by low UAM energy, which correlated to the peeling load and LWD.

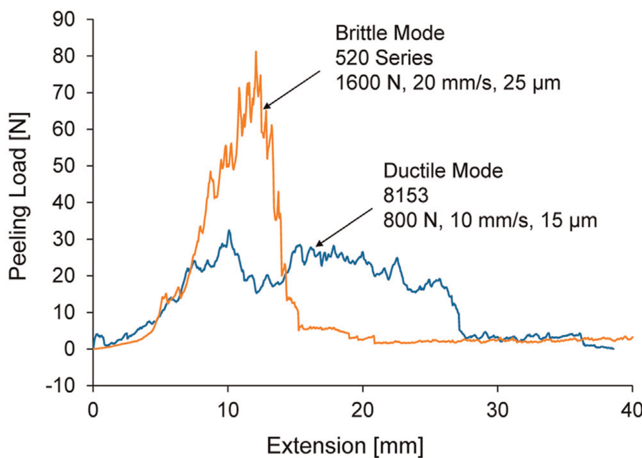

Fig. 10. Peeling profile of two kinds of fragile mode: brittle mode and ductile mode.

3.4. Effect of dielectric hardness on mechanical strength

According to Figs. 9 and 12, mechanical strength of UAM embedding was enhanced following the increase of dielectric hardness. This phenomenon probably referred to the deformation of dielectric film caused by UAM processing stress. During UAM embedding, harder dielectrics like 520 Series had a higher resistance to deformation when the UAM loading was applied, so the shape of dielectric film could be maintained and minimal dielectric material was squeezed to the adjacent regions (Fig. 14(a)). On the contrary, softer dielectrics such as 8153 were deformed into the Al–Al bonding area which decreased LWD and peel load (Fig. 14(b)). Accordingly, compared with a softer dielectric, harder dielectric had a restricted WEA and a higher LWD. As shown in Figs. 12 and 13, with high UAM energy 520 Series showed 4.7 mm

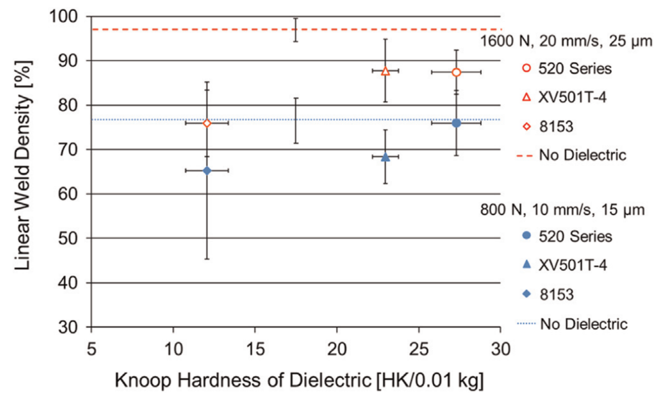

Fig. 12. Linear weld density for three dielectric films embedded with two combinations of UAM parameters.

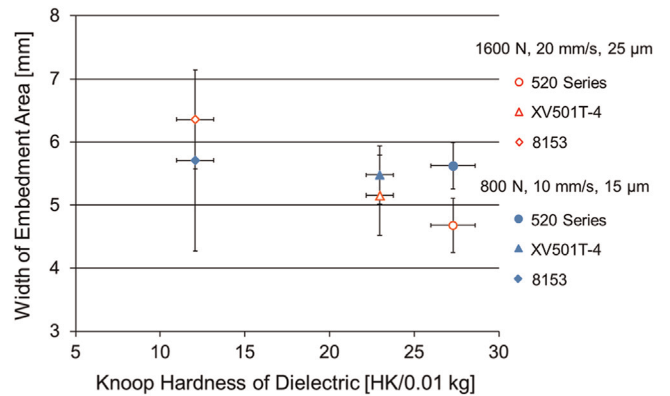

Fig. 13. Width of embedment area for three dielectric films embedded with two combinations of UAM parameters.

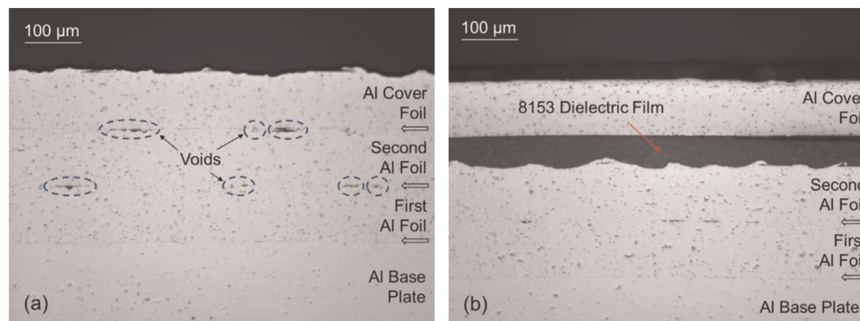

Fig. 11. (a) Cross-section of Al–Al weld interface; (b) Embedded 8153 dielectric film.

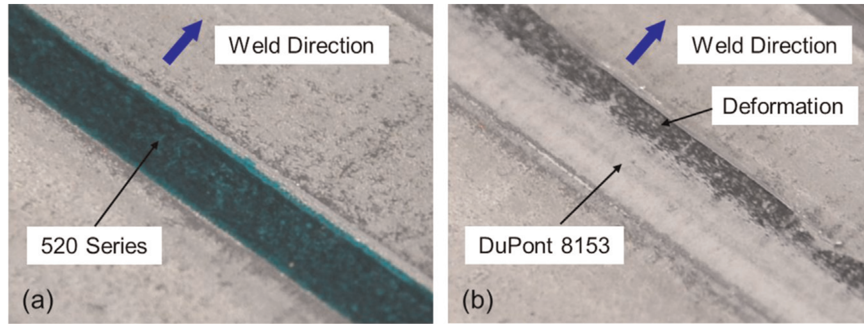

Fig. 14. Surface profile of embedded 520 Series (a) and 8153 (b) after Al cover foils were tore off (UAM settings: 1600 N weld force, 25 μm sonotrode amplitude, and 20 mm/s welding speed).

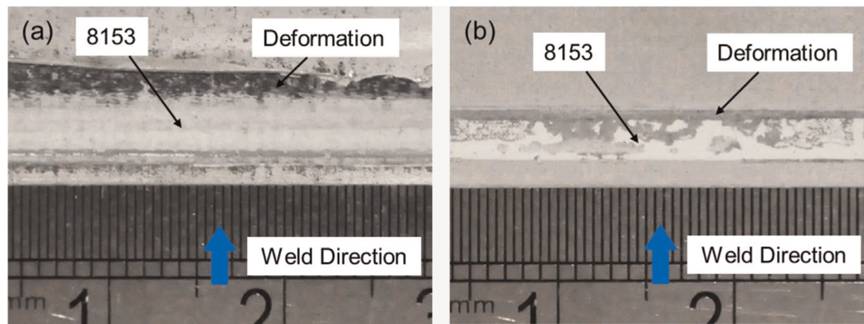

Fig. 15. 8153 dielectric film embeded by high (a) and low (b) UAM energy settings.

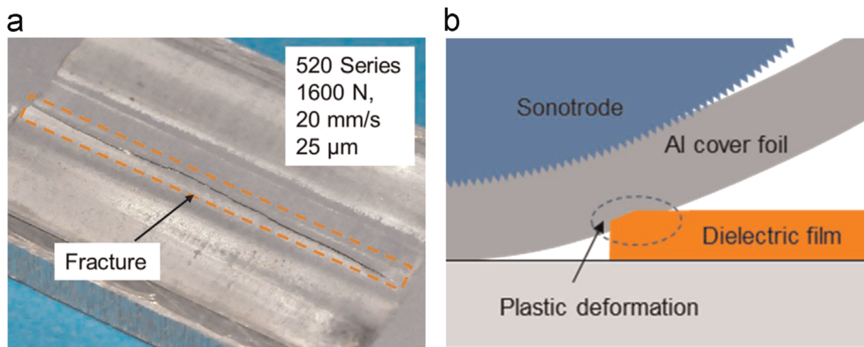

Fig. 16. (a) Fracture on the Al cover foils along the front edge of dielectric films; and (b) Schematic drawing of the mechanism of fracture formation.

WEA and 87% LWD compared with 6.4 mm WEA and 76% LWD of 8153. Both led to an obvious peeling load difference in Fig. 9.

Softer dielectrics (e.g. 8153) were squashed and deformed further along the Al–Al weld area as shown in Fig. 14(b). With higher UAM embedding energy 8153 was deformed and squeezed along the welding direction (Fig. 15(a)). This resulted in a large WEA (up to approx. 6.4 mm) and a reduction of LWD (by approx. 20% compared with the reference line) as shown in Figs. 12 and 13. Due to sufficient UAM processing energy, the deviations of WEA and LWD could be restricted. However, in the case of lower UAM energy, although the increase of WEA was not as much as the higher energy situation, a relatively large deviation (about 1.4 mm) was found in Fig. 13 and a significant deviation of LWD (about 20%) also occurred in Fig. 12. These were probably caused by the low UAM processing energy that was unable to induce sufficient deformation of the Al cover layer to adapt to the dielectric material deformation (Fig. 15(b)). In both cases, the 'squashing' of the dielectric layer caused mechanical strength degradation of the UAM embedded structure as shown in Fig. 9.

The dielectric film is vital for embedding electronics into metal matrices as it provides electrical insulation and mechanical resistance to external stress for the encapsulated conductive structure. Therefore the dielectric film must have sufficient hardness to withstand the stresses of the manufacturing process and the practical application.

3.5. Effect of UAM parameters on mechanical strength

Peel testing and cross-sectional analysis of the samples showed a trend that the mechanical strength of the UAM metal structures could be enhanced by using a derived combination of UAM parameters generating high processing energy.

However, large UAM energy could also result in deformation of the softer dielectric films as discussed above and additionally create fractures on the Al cover foil. For all three dielectrics, fractures were found on the Al cover foils of some samples along the front edge of dielectric films (Fig. 16(a)). During the UAM embedding, when the sonotrode pressed onto the front edge of the dielectric film, the sharp corner of the dielectric was flattened and modified to a slope. As the slope corner was deformed it imparted a groove on the

underside of the foil. Meanwhile, the rough UAM sonotrode surface was embossed onto the upper surface of the foil. Both the grooving and embossing made the Al foil more vulnerable and acted as a stress raiser in the foil structure (Fig. 16(b)). The deformation of the Al foil may have also been exaggerated and aggravated by the ultrasonic softening phenomenon [23] however more investigation would be necessary to confirm this. As the sonotrode continued its motion up and over the dielectric material, there would be no metallurgical bonding between the interface of the dielectric film and the Al foil. Therefore, the mechanical impedance to the Al cover foils motion drops rapidly, and the Al foil is then cyclically oscillated by the sonotrode with relatively larger amplitude compared to the surrounding bonded foil. The shear stress accumulated on the deformed cross-section, exceeding the shear yield strength of Al foil, and resulting in fracture along the front edge of the dielectric film. This is a new observation that has not been noted in previous research. This is likely due to previous embedding work focussing on mostly round edged hard articles such as SiC and optical fibres with associated small volumes (Typical diameters of these fibres are in the scale of 100–150 μm.).

3.6. Effect of surface roughness of aluminium substrate on mechanical strength

To achieve compact embedding of electrical components and enhance the integration of the metal matrix composite, the total thickness of the electrical structure needs to be limited. According to Table 4 and Fig. 6, it was found that the thickness of the electrical structure was largely determined by the roughness of the UAM processed Al substrate. The dielectric film must have been of sufficient thickness so that electrical insulation could be realised. Therefore, if the substrate could be fabricated smoother, the device thickness requirements will likely be decreased. By machining the UAM processed substrate a smoother surface can be made for the following printing process. This method will be investigated in future work, which is also attractive for improving mechanical strength of the UAM composites with embedded electrical pathways.

4. Conclusions and future work

This work investigated the feasibility of directly embedding dielectric materials within solid state additively manufactured metal matrices.

Three dielectric materials were successfully deposited and embedded demonstrating the compatibility of the dielectric films with the UAM process. The dielectric film adequately adapted to the inherent roughness of the Al substrate to provide full electrical insulation. During UAM embedding, the harder dielectric structures exhibited sufficient strength to withstand the mechanical stress during UAM processing, which is desirable for protecting future electrical conductive structures.

Peel testing and cross-sectional microscopy found that the mechanical strength of the dielectric embedded samples increased with the hardness of the dielectric material. The deformation of the dielectric film caused by UAM processing was found to be the reason. The ‘squash’ of dielectric material enlarged the embedding region and affected the average LWD resulting in a decrease of composite mechanical strength. For each dielectric, it was also observed that mechanical strength was improved by using higher UAM processing energy.

In the future, the mechanism of the fracture in the Al cover layer will be investigated further to improve mechanical strength. Furthermore, electrically conductive structures will be deposited and encapsulated within the dielectric film to build functional electrical devices such as strain gauges and heaters. The whole device then could be encased by UAM to realise multifunctional metal matrix composites.

Acknowledgement

This work was supported by the Engineering and Physical Sciences Research Council, UK via the Centre for Innovative Manufacturing in Additive Manufacturing, grant number EP/I033335/2.

References

[1] D.R. White, Adv. Mater. Process. 161 (2003) 64–65.
[2] C.Y. Kong, R.C. Soar, P.M. Dickens, Proc. Inst. Mech. Eng. Part C: J. Mech. Eng. Sci. 219 (2005) 83–91.
[3] S. Koellhoffer, J.W. Gillespie, S.G. Advani, T.A. Bogetti, J. Mater. Process. Technol. 211 (2011) 1864–1877.
[4] Y. Yang, G.D. Janaki Ram, B.E. Stucker, J. Mater. Process. Technol. 209 (2009) 4915–4924.
[5] C.Y. Kong, R. Soar, Appl. Opt. 44 (2005) 6325–6333.
[6] C. Mou, P. Saffari, D. Li, K. Zhou, L. Zhang, R. Soar, I. Bennion, Meas. Sci. Technol. 20 (2009) 034013.
[7] E. Siggard, A. Madhusoodanan, in: Proceedings of the 17th Annual Solid Freeform Fabrication Symposium University Texas Austin, Austin, TX, 2006, pp. 70–83.
[8] C.J. Robinson, B. Stucker, A.J. Lopes, R.B. Wicker, J.A. Palmer, in: Proceedings of the 17th Annual Solid Freeform Fabrication Symposium University Texas Austin, Society of Manufacturing Engineers, Austin, TX, 2006, pp. 60–69.
[9] Smith Metal, Sheet Metalwork Aluminium 1050A (S1B), Technic Data Sheet, 2003.
[10] MatWeb Material Property Data. 〈http://www.matweb.com/search/DataSheet.aspx?MatGUID=91c99440833341fc8fbe1d26149bc35e〉.
[11] DuPont Company, DuPont™ LuxPrint® 8153 Electroluminescent Material, Technic Data Sheet, 2009.
[12] Technic Company, 520 Series Thermal 2 Pack Solder Resists, Technic Data Sheet, 2008.
[13] SunChemical Company, ImagecureSMART® XV501T-4 ScreenTechnic Data Sheet, 2011.
[14] G.D. Janaki Ram, Y. Yang, B.E. Stucker, J. Manuf. Syst. 25 (2006) 221–238.
[15] C. Kong, R. Soar, P. Dickens, J. Mater. Process. Technol. 146 (2004) 181–187.
[16] M. Kulakov, H.J. Rack, J. Eng. Mater. Technol. 131 (2009) 021006.
[17] Y. Yang, G.D.J. Ram, B.E. Stucker, Rapid Prototyp. J. 16 (2010) 20–28.
[18] W.W. Walker, in: Proceedings of Microindentation Techniques in Materials Science and Engineering A: Symposium Sponsored by ASTM Committee E-4 on Metallography and by the International Metallographic Society, 1986, pp. 286–289.
[19] I.S. Goldstein, J. Vac. Sci. Technol. 20 (1982) 327–330.
[20] P. Fink-Jensen, Pure Appl. Chem. 10 (1965) 239–292.
[21] M. Ohring, Materials Science of Thin Films, Academic Press, United States, 2001 (ISBN 0080491782, 9780080491783).
[22] N. Gitis, I. Hermann, in: Proceedings of the 3rd Vienna International Conference Nanotechnology, 2009, pp. 225–229.
[23] B. Langenecker, IEEE Trans. Sonics Ultrason. 13 (1966) 1–8.